The Magnetic Rayleigh-Taylor Instability

by

Kain Chambers, BE BSc (Hons.)

Submitted in fulfilment of the requirements

for the degree of Doctor of Philosophy

School of Mathematics and Physics

University of Tasmania

November 2012

Acknowledgements

I would like to thank my supervisor Larry Forbes for his contributions, patience, understanding and enthusiasm.

Many staff from the UTAS Maths and Physics department deserve mention, namely, Karen Bradford, Michael Brideson, John Dickey, Kym Hill and my colleague Jacko for making the office a fun place to be.

I am also grateful to Raghvendra Sahai, John Trauger, the WFPC2 science team, NASA, ESA, The Hubble SM4 ERO Team and Robert Gendler for granting permission to publish the images in figures 4.2, 4.7 and 4.14(a), which may be found from the NASA public websites [52, 45, 46].

Finally, I would like to thank my family and friends for their assistance during this long endeavour.

I declare that this thesis contains no material which has been accepted for a degree or diploma by the University or any other institution, except by way of background information and duly acknowledged in the thesis, and to the best of my knowledge and belief no material previously published or written by another person except where due acknowledgement is made in the text of the thesis, nor does the thesis contain any material that infringes copyright.

Signed: 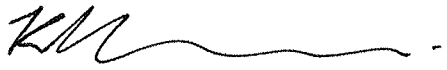

Kain Chambers

Date: 12/11/2012

This thesis may be made available for loan and limited copying and communication in accordance with the Copyright Act 1968.

Signed: 

Kain Chambers

Date: 12/11/2012

The following people contributed to the publication of work undertaken as part of this thesis.

The magnetic Rayleigh-Taylor instability for inviscid and viscous fluids [11]
Kain Chambers (80%), Larry Forbes (20%)

The cylindrical magnetic Rayleigh-Taylor instability for viscous fluids [12]
Kain Chambers (80%), Larry Forbes (20%)

We the undersigned agree with the above stated proportion of work undertaken for each of the above published (or submitted) peer-reviewed manuscripts contributing to this thesis.

Signed: Larry Forbes.

Larry Forbes
Supervisor
School of Mathematics and Physics
University of Tasmania

Date: 12 Nov. 2012.

Signed: John Dickey

John Dickey
Head of School
School of Mathematics and Physics
University of Tasmania

Date: 12 Nov 2012

Abstract

The Rayleigh-Taylor instability (RTI) arises whenever two fluids with different densities are arranged such that the heavier fluid sits above the lighter fluid, with a sharp interface in between. The magnetic Rayleigh-Taylor instability (MRTI) has the further complication due to the presence of a magnetic field throughout both media. The two fluids in question may also have differing magnetic properties, such as the magnetic permeability. When the fluids in consideration are in fact plasmas comprised of charged particles, induced currents, magnetic fields and Lorentz forces can all act in ways that will affect the stability of the system.

The RTI has widespread applications in atmospheric physics, oceanography, meteorology, laboratory plasma physics, nuclear reactors, inertial confinement fusion as well as the field of astrophysics, where the instability plays an important role in supernova explosions, accretion discs, plasma jets and H II regions (clouds of gas in which star formation has recently taken place) amongst others. It is closely related to two other hydrodynamic instabilities, namely the Kelvin-Helmholtz instability (KHI) and the Richtmyer-Meshkov instability (RMI).

This thesis considers in detail several different flow configurations in which the RTI arises. A key feature of these configurations is that small wavelike disturbances to the flow are unstable. These configurations are studied to determine the behaviour of these unstable flows. A particular focus is the effects due to the presence of a magnetic field, and the mechanisms that alter the flow in the magnetic case.

The thesis begins by considering two dimensional planar flow in Cartesian geometry in which the amplitude of the waves is small compared with their wavelength. The flow is assumed to be incompressible and inviscid. In this scenario, linear theory is used to derive a closed form solution for the evolution of the interface between the two fluids. This solution shows quantitatively how the position of the interface depends on the ratio of the densities of the two

fluids, the wavelength of the disturbance, as well as the strength and direction of the applied magnetic field.

The unstable nature of the RTI means that after some finite time, the amplitude of the waves will grow to a size comparable with their wavelength, and in this scenario, linear theory is not appropriate. For this reason, a non-linear model is considered, again for two dimensional planar flow in Cartesian geometry. The flow in this case is considered to be weakly compressible, and viscous. Results in the non-linear case are obtained by use of a combination of streamfunction, spectral and finite difference techniques. The results show qualitatively various non-linear phenomena such as interface roll-up, fingering and bubble formation. It is shown in particular how different initial conditions give rise to outcomes that are very different in terms of the geometry of the interface between the two fluids, primarily the differences between a single mode disturbance and a multi mode disturbance to the interface at time $t = 0$.

The final problem studied in this thesis considers two dimensional flow in circularly symmetric cylindrical geometry. The configuration in this case is comprised of a heavy fluid surrounding a light fluid, and gravity is directed radially inwards. A massive object is located at the centre of the light fluid, and it behaves like a line dipole both for fluid flow and magnetic field strength. In the non-linear, weakly compressible, viscous regime, the initially circular interface between the two conducting fluids evolves into plumes, dependent on the magnetic and fluid dipole strengths and the nature of the initial disturbance to the interface. A spectral method is presented to solve the time-dependent interface shapes, and results are presented and discussed. Bipolar solutions are possible, and these are of particular relevance to astrophysics. The solutions obtained resemble structures of some HII regions and nebulae.

Contents

List of Figures

Chapter 1

Introduction

The study of instabilities in fluids is a vast field of active research. Typically, an instability occurs when a stable base flow is perturbed. Various types of instabilities are possible, a few common examples being the Kelvin-Helmholtz [35, 29] instability (KHI), the Richtmyer-Meshkov [51, 41] instability (RMI) and the Rayleigh-Taylor [50, 59] instability (RTI), which are named after the pioneer researchers in each case. These instabilities are closely related, in that they all share some common features, and it is possible in some circumstances that these instabilities occur simultaneously. In each case, a number of fluids is present and of particular interest is the behaviour of an interface that separates two fluids. The configuration for an unstable RTI requires the heavier of the two fluids to be located at a region of higher gravitational potential than the lighter fluid. In general, the fluids may be subject to any acceleration, not necessarily gravitational, but in many applications the acceleration is indeed due to gravitational forces. The RTI differs from the KHI, in which the relative velocity difference at the interface is responsible for unstable flow, and the RMI which requires impulsive acceleration such as a shock wave at the interface. It is the magnetic RTI (MRTI) that is the topic of this thesis. This version of the instability includes the presence of magnetic fields, and considers various electro-magnetic effects such as conductivity, induced currents, Lorentz forces

and magnetic permeability. The inclusion of these additional effects typically results in a flow that is less unstable than the non-magnetic equivalent, specifically in that the growth rate of the instability is suppressed. The MRTI has applications in a range of scales from laboratory plasma physics to atmospheric physics and astrophysics.

A common question that arises in the study of a fluid instability concerns the conditions for an interface between two fluids to be stable. The growth rate of an arbitrary disturbance and hence the stability of the system will depend in general on some combination of the properties of that system. Frequently, for wave-like disturbances in the linear scenario, the stability of a disturbance can be shown to be dependent on the wavelength of that disturbance by use of a common linearisation technique. This functional quantity is known as a dispersion relation, and it applies at early times during the instability where the amplitude of the waves is smaller than their wavelength. The growth rate of the interface for the linear regime in the magnetic free case is a classic result. Taylor [59] showed that this rate depends only on the densities of the two fluids, the well known Atwood number. The presence of a base magnetic field complicates matters somewhat. In 1961, Chandrasekhar [13] derived the form of the growth rate for fluids that are incompressible, inviscid, stratified and have zero resistivity. This rate depends not only on the densities of the fluids, but also on the strength and direction of the base magnetic field. Chapter two of this thesis contains a derivation of the linearised growth rate for the MRTI, under slightly different conditions than those used by Chandrasekhar.

The question of stability is naturally extended to such cases where non-linear effects contribute to the flow. These will typically be significant for modes where the wave amplitude has grown to be large compared with its wavelength and hence the approximations used in the linearised analysis become invalid. Compressibility, viscosity and Lorenz forces in the magnetic case are examples of effects that can be considered in the non-linear regime. The non-linear growth of disturbances is the topic of the third chapter of this thesis. Due to the

intractability of analytic solutions for a non-linear system of partial differential equations (PDEs), one naturally considers some type of numerical scheme to solve for the flow within some appropriate computational boundary. Such schemes are still an active area of research. A common and reasonably stable method, in particular for the two dimensional Cartesian geometry considered here, for solving such a non-linear system of PDEs is the Alternating Direction Implicit (ADI) method [31]. Such a method is unsuitable in the case of the MRTI however, given that we cannot maintain the divergence free nature of the magnetic field exactly by use of any purely numerical scheme. This is a critical fact, since it was shown by Brackbill and Barnes [9] that a small numerical error in this quantity results in an effect equivalent to a fictitious force parallel to the magnetic field. Such a force is quite undesirable, and hence it is essential to avoid such a situation. Various so called constrained transport algorithms have been designed and implemented in a range of works, for example Isobe et. al [32], Stone and Gardiner [57] and Jun et.al [33], to accomplish this task. These algorithms require some additional assumptions and approximations in order to maintain a divergent free magnetic field. Some examples are the algorithms CANS [38], FLASH [15], WP/PPM [60] and ZEUS-3D [55]. A different approach was taken in this thesis, whereby a combination of spectral and finite difference techniques is performed. The two dimensional flow is solved by use of spectral techniques in one of the dimensions, and by finite difference techniques in the other dimension. Rather than solving for the numerical values of the flow quantities directly as for a purely numerical scheme, each quantity is represented in spectral form as an analytic series, and it is the coefficients of these series that are solved for numerically by use of the Crank-Nicolson finite difference scheme. An appropriate choice for the form of each series in conjunction with a stream function approach ensures that the divergence free nature of the magnetic field is satisfied exactly. This method has two key advantages; firstly, the resulting system of equations is tri-diagonal, meaning that computationally expensive matrix inversion techniques can be avoided, and secondly,

the additional assumptions and approximations used by the above constrained transport algorithms are not required. The stream function and associated vorticity approach is particularly convenient in view of work by Forbes [24] where it was shown that fluid vorticity is the mechanism for interface roll-up, and in this present work where it is shown that magnetic vorticity is the mechanism for growth suppression.

Chapter four of this thesis is devoted to a study of the MRTI in cylindrical geometry in two dimensions with circular symmetry. The presence of curved geometry causes additional effects that have no equivalent in the flat, Cartesian geometry. The curvature of the space affects the stability of the system, and this is known as the Bell-Plesset effect, since Bell [8] was the first to discover this result for cylindrical geometry, while a short time later Plesset [49] achieved a similar result for spherical geometry. The convergent nature of cylindrical geometry requires one to also consider how to represent the center of the compressing fluid. In reality, the pressure must remain finite as the radius approaches zero. As discussed in a paper by Epstein, [20], in order to conserve mass, there must be some small central volume with appropriate properties to compensate for these constraints. A line source is such a volume in the limit that the volume tends to zero. This representation is appropriate and mathematically convenient. Due to the already discussed divergence free nature of the magnetic field however, we are forced to use a higher order singularity in this paper, a line dipole to model this small volume. As for the case in Cartesian geometry, a numerical scheme is required to solve for the flow. Ignoring for the moment the aforementioned fact that purely numerical schemes are inappropriate in the case of the MRTI, it is remarked that the use of a finite difference scheme would not be straightforward in any case given the presence of dipole type singularities at the origin. The approach taken in this thesis is to use spectral techniques in both the radial and azimuthal dimensions. The dipole nature of both the fluid flow and magnetic field is satisfied exactly using an appropriate representation. In addition, the values of all quantities on the computational boundary are

straightforward. The use of the spectral method results in a system of ordinary differential equations (ODEs) for the coefficients of the various series representations. This is integrated forwards in time using the classic Runge-Kutta RK4 method [5], which is stable for appropriately small time steps. It is observed that a single mode initial disturbance of an integer wave number gives rise to the formation of that integer number of plumes. In view of this observation, the focus of the work of this chapter is on bipolar solutions given the interest of such phenomena in astrophysics, the study of plasma jets, HII regions and nebulae being examples. A small section that considers other such possibilities, for example, tri-polar plumes is also presented. The results are compared with real observations of such structures and demonstrate how magnetic effects alter the development of the RTI in the given geometry. The resulting flows are shown to be highly dependent on a dimensionless quantity called the magnetic Froude number. Comparisons are made with the magnetic free regime, and the underlying mechanisms that alter the evolution of the flow in the magnetic case are presented and discussed.

Chapter 2

An analytic method for the time evolution of interfacial waves of a two fluid magnetic Rayleigh-Taylor configuration in the small amplitude approximation

2.1 Introduction

The classic Rayleigh-Taylor problem was first studied by Lord Rayleigh in 1883 [50], and Sir G.I. Taylor in 1950 [59]. Taylor's analysis assumed the waves at the interface were small, and he applied linear theory to obtain an exponential growth rate for the interface. The magnetic case was studied analytically by

Chandrasekhar in 1961 [13] for fluids that are incompressible, inviscid, stratified and have zero resistivity. Chandrasekhar showed how the presence of a background magnetic field altered Taylor's growth rate, again in the linear regime. The MRTI instability is also known as the Parker Instability, due to work by Parker in 1966 [48], in which the MRTI was suggested to be responsible for various observed astrophysical effects, such as the concentration of the interstellar plasma into discrete clouds.

The purpose of this introductory chapter is to derive the analytic form for the growth rate of the interface between two fluids in the linear regime for the MRTI. It will be shown that this quantity depends on the ratio of the densities of the two fluids and the base magnetic field strength. The result is in agreement with earlier work by Chandrasekhar [13] in which a different approach to the present work was taken. This analytic result is essential in order to understand the behaviour of the system at early times where the wave amplitude is much smaller than the wavelength. From the analytic nature of the result, it can be concluded that there are three possible qualitatively different behaviours for the flow. The main discussion concerns the role that magnetic effects have on the flow, and it is shown how the flow can be either stable, unstable or oscillatory in nature depending on the strength and direction of the base magnetic field. These behaviours are of use in conjunction with work in later chapters of this thesis that consider the MRTI in the non-linear regime. The results in the non-linear regime are of a numerical nature, and hence a comparison with the analytic results at early times gives confidence that the numeric techniques are stable and accurate.

The remainder of the chapter is structured as follows. After presenting the magnetohydrodynamical model for the system, the analytic time dependent solution for the interface is obtained for the two geometrically different cases of firstly, a horizontal base magnetic field, and secondly, for a vertical base magnetic field. The solution approaches and results have significant differences, hence the separate treatments. Finally, due to the linear nature of the assumed

solutions, it is an elementary calculation to obtain the solution for the interface in the case of an arbitrarily directed base magnetic field by use of the superposition principle. To conclude, some consequences of certain parameter combinations are discussed, along with a comparison of the obtained solution with the well known Atwood number in the case of the magnetic free RTI.

2.2 Model and Governing Equations

We begin by considering the two dimensional case of two incompressible, inviscid fluids separated by a sharp interface. Following the notation of Batchelor [6], the upper and lower fluids are denoted by layers 2 and 1 respectively. The upper fluid has density ρ_2 and magnetic permeability $\mu_2 = 1$, while the lower fluid has density ρ_1 and magnetic permeability $\mu_1 = 1$. In the case of interest, the upper fluid is heavier, hence we have $\rho_2 > \rho_1$. The upper and lower fluid meet at an interface denoted by $z = \eta(x,t)$. Flow is assumed to be periodic in the horizontal x coordinate, with period λ, while the vertical z direction extends indefinitely. The gravitational body force is described by $-g\hat{\boldsymbol{e}}_{\boldsymbol{z}}$.

We start with the governing MHD equations for this scenario, which in each of the two incompressible media comprise conservation of mass,

$$\nabla \cdot \boldsymbol{v} = 0, \tag{2.1}$$

and conservation of momentum with both gravitational and magnetic body forces,

$$\rho\left[\frac{\partial \boldsymbol{v}}{\partial t} + (\boldsymbol{v}\cdot\nabla)\,\boldsymbol{v}\right] + \nabla p^* = \frac{1}{\mu}(\boldsymbol{B}\cdot\nabla)\,\boldsymbol{B}, \tag{2.2}$$

where $p^* = p + \rho g z + B^2/(2\mu)$.

Next, we have an absence of magnetic monopoles,

$$\nabla \cdot \boldsymbol{B} = 0 \tag{2.3}$$

and Faraday's Law,

$$\frac{\partial \boldsymbol{B}}{\partial t} = -\nabla \times \boldsymbol{E}.$$

We substitute the Lorentz equation $\boldsymbol{J} = \sigma\left(\boldsymbol{E} + \boldsymbol{v} \times \boldsymbol{B}\right)$ as well as Ampere's Law $\boldsymbol{\nabla} \times \boldsymbol{B} = \mu \boldsymbol{J}$ into Faraday's Law and make use of the vector identity $\nabla \times (\nabla \times \boldsymbol{B}) = \nabla\left(\nabla \cdot \boldsymbol{B}\right) - \nabla^2 \boldsymbol{B}$ to obtain

$$\frac{\partial \boldsymbol{B}}{\partial t} = \nabla \times (\boldsymbol{v} \times \boldsymbol{B}) + \frac{1}{\mu\sigma}\nabla^2 \boldsymbol{B}. \tag{2.4}$$

Under the assumption of infinitely conducting media, $\sigma \to \infty$, Faraday's Law is simply

$$\frac{\partial \boldsymbol{B}}{\partial t} - \nabla \times (\boldsymbol{v} \times \boldsymbol{B}) = \boldsymbol{0}. \tag{2.5}$$

The unit normal to the interface is found by taking the gradient of the level surface representing the interface. This gives

$$\hat{\boldsymbol{n}} = \frac{-\left(\partial\eta/\partial x\right)\hat{\boldsymbol{e}}_{\boldsymbol{x}} + \hat{\boldsymbol{e}}_{\boldsymbol{z}}}{\sqrt{1 + \left(\partial\eta/\partial x\right)^2}}. \tag{2.6}$$

We use equations (2.1), (2.2), (2.3) and (2.5) in conjunction with (2.6) to derive the conditions at the interface between our two fluids. The velocity and magnetic field vectors have components $\boldsymbol{v} = (u, 0, w)$ and $\boldsymbol{B} = (B_x, 0, B_z)$ respectively, and a subscript number is used to indicate in which medium, 1 or 2, the quantity applies. From the conservation of mass (2.1), we require that the normal component of the velocity of the fluid in each medium be equal to the normal velocity of the interface, that is,

$$-u_1 \frac{\partial \eta}{\partial x} + w_1 = -u_2 \frac{\partial \eta}{\partial x} + w_2 = \frac{\partial \eta}{\partial t} \quad \text{on } z = \eta. \tag{2.7}$$

Next, from the absence of magnetic monopoles (2.3), we require the normal component of the magnetic field in each fluid to be equal,

$$-B_{x_1} \frac{\partial \eta}{\partial x} + B_{z_1} = -B_{x_2} \frac{\partial \eta}{\partial x} + B_{z_2} \quad \text{on } z = \eta. \tag{2.8}$$

The Faraday equation (2.5) implies that the tangential components of the electric field $\boldsymbol{E} = -\boldsymbol{v} \times \boldsymbol{B}$ in each fluid are equal, or $\hat{\boldsymbol{n}} \times (\boldsymbol{E_2} - \boldsymbol{E_1}) = \boldsymbol{0}$ at the interface. This is expressed in the form

$$w_1 B_{x_1} - w_2 B_{x_2} = u_1 B_{z_1} - u_2 B_{z_2} \quad \text{on } z = \eta. \tag{2.9}$$

Finally, from the momentum vector equation (2.2), by Newton's Third Law we need the forces on each side of the surface of the interface to be equal and opposite, and we obtain two conditions, one for each component of the equation,

$$\begin{aligned}
&\left(\rho_1 u_1^2 + p_1^* - \frac{B_{x_1}^2}{\mu_1}\right)\left(\frac{-\partial\eta}{\partial x}\right) + \left(\rho_1 u_1 w_1 - \frac{B_{x_1} B_{z_1}}{\mu_1}\right) = \\
&\left(\rho_2 u_2^2 + p_2^* - \frac{B_{x_2}^2}{\mu_2}\right)\left(\frac{-\partial\eta}{\partial x}\right) + \left(\rho_2 u_2 w_2 - \frac{B_{x_2} B_{z_2}}{\mu_2}\right) \quad \text{on } z = \eta \\
&\left(\rho_1 u_1 w_1 - \frac{B_{x_1} B_{z_1}}{\mu_1}\right)\left(\frac{-\partial\eta}{\partial x}\right) + \left(\rho_1 w_1^2 + p_1^* - \frac{B_{z_1}^2}{\mu_1}\right) = \\
&\left(\rho_2 u_2 w_2 - \frac{B_{x_2} B_{z_2}}{\mu_2}\right)\left(\frac{-\partial\eta}{\partial x}\right) + \left(\rho_2 w_2^2 + p_2^* - \frac{B_{z_2}^2}{\mu_2}\right) \quad \text{on } z = \eta.
\end{aligned} \tag{2.10}$$

We now introduce new dimensionless variables and coordinates, with characteristic length $\lambda/2\pi$ and characteristic time $\sqrt{\lambda/2\pi g}$ as in Forbes [24]. In these dimensionless variables, the flow has period 2π in x, the characteristic speed is given by $\sqrt{\lambda g/2\pi}$, while the reference pressure, magnetic flux density and current density work out to be $\rho_1 \lambda g/2\pi$, $\sqrt{\mu_1 \lambda \rho_1 g/2\pi}$ and $\sqrt{2\pi\rho_1 g/\mu_1 \lambda}$ respectively. Finally, the gravitational body force is described by $-\hat{\boldsymbol{e}}_{\boldsymbol{z}}$. In this dimensionless scheme, there is one parameter, D, which is the ratio ρ_2/ρ_1, and we have $\mu_1 = \mu_2 = 1$. The system of equations in dimensionless variables for the two media, 1 and 2, require minimal adjustment from equations (2.1), (2.3) and (2.5); only the additions of the subscripts for each medium is required. The dimensionless momentum equations (2.2), however, are modified slightly,

becoming,

$$\begin{aligned}\frac{\partial \boldsymbol{v_1}}{\partial t} + (\boldsymbol{v_1}\cdot\nabla)\,\boldsymbol{v_1} + \nabla p_1^* &= (\boldsymbol{B_1}\cdot\nabla)\,\boldsymbol{B_1}\\ \frac{\partial \boldsymbol{v_2}}{\partial t} + (\boldsymbol{v_2}\cdot\nabla)\,\boldsymbol{v_2} + \frac{1}{D}\nabla p_2^* &= \frac{1}{D}\,(\boldsymbol{B_2}\cdot\nabla)\,\boldsymbol{B_2},\end{aligned} \tag{2.11}$$

where $p_1^* = p_1 + z + B_1^2/2$ and $p_2^* = p_2 + Dz + B_2^2/2$.

At the interface between the two fluids, the conditions in dimensionless variables take the same form as equations (2.7), (2.8) and (2.9), while the momentum conditions (2.10) become

$$\begin{aligned}\left(u_1^2 + p_1^* - B_{x_1}^2\right)\left(\frac{-\partial\eta}{\partial x}\right) + \left(u_1 w_1 - B_{x_1}B_{z_1}\right) &=\\ \left(Du_2^2 + p_2^* - B_{x_2}^2\right)\left(\frac{-\partial\eta}{\partial x}\right) + \left(Du_2 w_2 - B_{x_2}B_{z_2}\right) &\quad \text{on } z=\eta.\\ \left(u_1 w_1 - B_{x_1}B_{z_1}\right)\left(\frac{-\partial\eta}{\partial x}\right) + \left(w_1^2 + p_1^* - B_{z_1}^2\right) &=\\ \left(Du_2 w_2 - B_{x_2}B_{z_2}\right)\left(\frac{-\partial\eta}{\partial x}\right) + \left(Dw_2^2 + p_2^* - B_{z_2}^2\right) &\quad \text{on } z=\eta.\end{aligned} \tag{2.12}$$

A sketch of the dimensionless flow situation is given in figure 2.1.

2.3 Small Amplitude Theory

As for the classical Rayleigh-Taylor problem, we perturb a stable base flow by introducing small amplitude waves of wavelength λ at the interface. It will be seen that these waves will grow in time due to the unstable configuration of the fluid. We consider two cases; the first case where the base magnetic field is parallel to the interface, and the second case where the base magnetic field is perpendicular to the interface. Since this small amplitude problem is linear, we may apply the super-position principle to solve for the response due to a base magnetic field at any angle relative to the interface.

A non-trivial stable 2D base flow that exists for this problem is given by $\boldsymbol{v_1} = \boldsymbol{v_2} = \boldsymbol{0}$, $\boldsymbol{B_1} = \boldsymbol{B_2} = \beta\,(l_x\hat{\boldsymbol{e}}_{\boldsymbol{x}} + l_z\hat{\boldsymbol{e}}_{\boldsymbol{z}})$, $p_1 = -z$, $p_2 = -Dz$ and $\eta = 0$. The dimensionless constant β represents the ratio of the base magnetic flux density

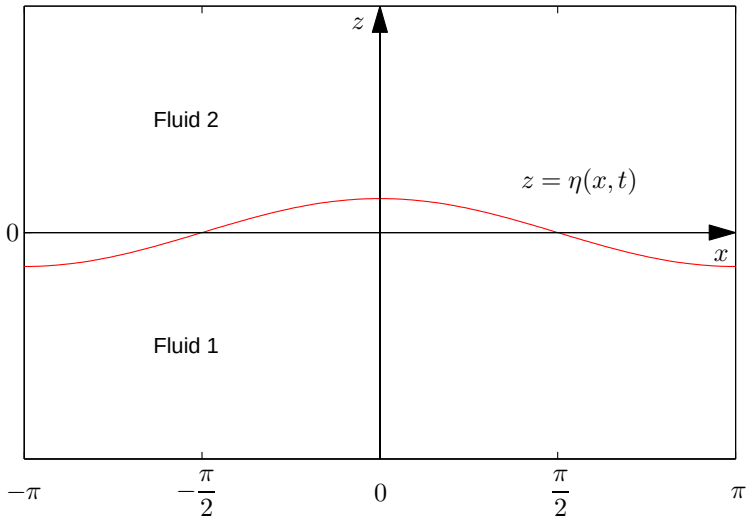

Figure 2.1: Configuration of the problem. A single disturbance of period 2π in x is shown.

to the reference flux density $\sqrt{\mu_1 \lambda \rho_1 g/2\pi}$. The quantities l_x and l_z are direction cosines, related by the condition

$$l_x^2 + l_z^2 = 1. \tag{2.13}$$

We are now ready to apply small perturbations of order ϵ to the above base flow, where a hat denotes a perturbed quantity except in the case of the unit vectors $\hat{\boldsymbol{e}}_{\boldsymbol{x}}$ and $\hat{\boldsymbol{e}}_{\boldsymbol{z}}$, but this should be clear from the context. The symbol $O\left(\epsilon^2\right)$ is used to represent additional terms of order epsilon squared. Our perturbed

quantities take the forms,

$$\begin{aligned}
\boldsymbol{v_1} &= \epsilon\, \hat{\boldsymbol{V}}_{\boldsymbol{1}} + O\left(\epsilon^2\right) \\
\boldsymbol{v_2} &= \epsilon\, \hat{\boldsymbol{V}}_{\boldsymbol{2}} + O\left(\epsilon^2\right) \\
\boldsymbol{B_1} &= \beta\left(l_x \hat{\boldsymbol{e}}_{\boldsymbol{x}} + l_z \hat{\boldsymbol{e}}_{\boldsymbol{z}}\right) + \epsilon \hat{\boldsymbol{B}}_{\boldsymbol{1}} + O\left(\epsilon^2\right) \\
\boldsymbol{B_2} &= \beta\left(l_x \hat{\boldsymbol{e}}_{\boldsymbol{x}} + l_z \hat{\boldsymbol{e}}_{\boldsymbol{z}}\right) + \epsilon \hat{\boldsymbol{B}}_{\boldsymbol{2}} + O\left(\epsilon^2\right) \\
p_1 &= -z + \epsilon \hat{P}_1 + O\left(\epsilon^2\right) \\
p_2 &= -Dz + \epsilon \hat{P}_2 + O\left(\epsilon^2\right) \\
\eta &= \epsilon \hat{H} + O\left(\epsilon^2\right). \qquad (2.14)
\end{aligned}$$

The model from section 2.2 is linearised about the interface $z = 0$ by use of equations (2.14), and we proceed to solve for $\hat{\boldsymbol{V}} = (\hat{u}, 0, \hat{w})$, $\hat{\boldsymbol{B}} = \left(\hat{b}_x, 0, \hat{b}_z\right)$, $\hat{P}$ and $\hat{H}$. It is clear that the conservation of mass and magnetic monopole equations remain unchanged in the linear regime. The linearised form of the momentum equations (2.11) becomes

$$\begin{aligned}
\frac{\partial \hat{\boldsymbol{V}}_{\boldsymbol{1}}}{\partial t} + \nabla \hat{P}_1 &= \beta\left[\left(\nabla \times \hat{\boldsymbol{B}}_{\boldsymbol{1}}\right) \cdot \hat{\boldsymbol{e}}_{\boldsymbol{y}}\right]\left(l_z \hat{\mathbf{e}}_x - l_x \hat{\mathbf{e}}_z\right) \\
\frac{\partial \hat{\boldsymbol{V}}_{\boldsymbol{2}}}{\partial t} + \frac{1}{D}\nabla \hat{P}_2 &= \frac{\beta}{D}\left[\left(\nabla \times \hat{\boldsymbol{B}}_{\boldsymbol{2}}\right) \cdot \hat{\boldsymbol{e}}_{\boldsymbol{y}}\right]\left(l_z \hat{\mathbf{e}}_x - l_x \hat{\mathbf{e}}_z\right),
\end{aligned}$$

while the linearised version of the Faraday equations (2.5) is given by

$$\begin{aligned}
\frac{\partial \hat{\boldsymbol{B}}_{\boldsymbol{1}}}{\partial t} &= \beta\left(l_x \frac{\partial \hat{\boldsymbol{V}}_{\boldsymbol{1}}}{\partial x} + l_z \frac{\partial \hat{\boldsymbol{V}}_{\boldsymbol{1}}}{\partial z}\right) \\
\frac{\partial \hat{\boldsymbol{B}}_{\boldsymbol{2}}}{\partial t} &= \beta\left(l_x \frac{\partial \hat{\boldsymbol{V}}_{\boldsymbol{2}}}{\partial x} + l_z \frac{\partial \hat{\boldsymbol{V}}_{\boldsymbol{2}}}{\partial z}\right).
\end{aligned}$$

The same process is used to linearise the interface conditions, (2.7)-(2.9) and

(2.12), resulting in,

$$\hat{w}_1 = \hat{w}_2 = \frac{\partial \hat{H}}{\partial t} \text{ on } z = \eta$$

$$\hat{B}_{z_1} = \hat{B}_{z_2} \text{ on } z = \eta$$

$$\beta l_z \hat{u}_1 = \beta l_z \hat{u}_2 \text{ on } z = \eta$$

$$\beta l_z \hat{B}_{x_1} = \beta l_z \hat{B}_{x_2} \text{ on } z = \eta$$

$$\hat{P}_1 + \beta l_x \hat{B}_{x_1} + (D-1)\hat{H} = \hat{P}_2 + \beta l_x \hat{B}_{x_1} \text{ on } z = \eta. \tag{2.15}$$

The next set of conditions is those that apply on the horizontal boundaries as $z \to \pm\infty$. The perturbation to the flow has no effect in these regions, resulting in the base flow conditions,

$$\hat{\boldsymbol{V}} \to \boldsymbol{0},\ \hat{\boldsymbol{B}} \to \boldsymbol{0},\ \hat{P} \to 0, \text{ as } z \to \pm\infty. \tag{2.16}$$

Due to the already mentioned assumptions that the initial perturbation to the stable base flow is a small amplitude sinusoidal wave of wavelength λ, the linear nature of the problem and the 2π-periodicity of the flow in the horizontal x-coordinate, we can represent the time-dependant perturbation to the interface in dimensionless variables by

$$\hat{H}(x,t) = \tilde{H}(t)\cos x. \tag{2.17}$$

The choice of the cosine function is somewhat arbitrary, the use of a sine function or a combination of sine and cosine functions would correspond to a shift of the origin in the horizontal x-coordinate. Finally, at time $t = 0$ the velocity of the fluid is zero and we set

$$\tilde{H}(0) = 1 \tag{2.18}$$

since this satisfies the assumption that the initial amplitude of the disturbing waves is ϵ. We now consider separate treatments for solving the equations for horizontal and vertical base magnetic fields.

2.3.1 Horizontal Base Field

The assumed nature of the perturbation to the interface (2.17) gives rise to a solution of the following form for the remaining perturbed quantities:

$$\begin{aligned}
\hat{u}(x,z,t) &= \tilde{u}(z,t)\sin x \\
\hat{w}(x,z,t) &= \tilde{w}(z,t)\cos x \\
\hat{P}(x,z,t) &= \tilde{P}(z,t)\cos x \\
\hat{b}_x(x,z,t) &= \tilde{b}_x(z,t)\cos x \\
\hat{b}_z(x,z,t) &= \tilde{b}_z(z,t)\sin x.
\end{aligned} \tag{2.19}$$

We seek a solution for $\tilde{w}(z,t)$ in each medium, since this then allows calculation of $\eta(x,t)$ by equations (2.19), (2.15), (2.18) and (2.14) respectively. The assumed forms (2.19) are substituted into the two linear systems of six first order partial differential equations (PDEs) developed in section 2.3 that describe the behaviour of the flow in each of media 1 and 2 respectively. One may eliminate all unknown quantities with the exception of $\tilde{w}(z,t)$ from the equation governing the x-component of momentum in each medium by the use of substitution and differentiation. It is now convenient to define the intermediate quantities $\tilde{M}$ and $\tilde{N}$ by,

$$\begin{aligned}
\tilde{M}(z,t) &= \frac{\partial^2 \tilde{w}_1}{\partial t^2} + \beta^2 \tilde{w}_1 \\
\tilde{N}(z,t) &= \frac{\partial^2 \tilde{w}_2}{\partial t^2} + \frac{\beta^2}{D}\tilde{w}_2.
\end{aligned} \tag{2.20}$$

The twelve PDEs developed in section 2.3 have thus been reduced to the following two second order PDEs for the intermediate quantities $\tilde{M}$ and $\tilde{N}$,

$$\begin{aligned}
\tilde{M} - \frac{\partial^2 \tilde{M}}{\partial z^2} &= 0 \\
\tilde{N} - \frac{\partial^2 \tilde{N}}{\partial z^2} &= 0.
\end{aligned} \tag{2.21}$$

Now we apply the separation of variables technique to equations (2.20) and (2.21) to obtain the following forms for the vertical velocities $\tilde{w}_1(z,t)$ and $\tilde{w}_2(z,t)$,

$$\begin{aligned}\tilde{w}_1 &= r_1 e^z \sinh s_1 t \\ \tilde{w}_2 &= r_2 e^{-z} \sinh s_2 t.\end{aligned} \tag{2.22}$$

We use the interface conditions (2.15), the boundary conditions (2.16) and the initial condition for the interface, (2.18) to solve for the constants r_1, r_2, s_1, s_2, and thus the velocities of the flow by equation (2.22). The pressures and magnetic flux densities then follow directly from the system of linearised PDEs. The quantity of main interest, however, is the profile of the interface,

$$\eta(x,t) = \epsilon \cosh\left(\sqrt{\mathcal{A}_{m_{||}}}t\right)\cos x + O\left(\epsilon^2\right), \tag{2.23}$$

where the magnetic Atwood number for the field parallel to the interface is given by

$$\mathcal{A}_{m_{||}} = \frac{D-1-2\beta^2}{D+1}. \tag{2.24}$$

It is trivial to see that in the absence of a magnetic field, we recover the well known Atwood number $\mathcal{A} = (D-1)/(D+1)$ as for the conventional RTI; see Forbes [24].

2.3.2 Vertical Base Field

As for the horizontal base field case, the perturbation to the interface is described by equation (2.17). In the present section considering a vertical base field, the form of the solution variables $\hat{u}$, $\hat{w}$ and $\hat{P}$ is the same as in equation (2.19). The

form of the magnetic flux densities is replaced with

$$\hat{b}_x(x,z,t) = \tilde{b}_x(z,t)\sin x$$
$$\hat{b}_z(x,z,t) = \tilde{b}_z(z,t)\cos x.$$

As for the horizontal scenario, it is convenient to define two intermediate quantities, in this case, $\tilde{K}$ and $\tilde{L}$, by

$$\tilde{K}(z,t) = \frac{\partial^2 \tilde{w}_1}{\partial z^2} - \tilde{w}_1$$
$$\tilde{L}(z,t) = \frac{\partial^2 \tilde{w}_2}{\partial z^2} - \tilde{w}_2.$$

Next, in a similar fashion as for the horizontal case, we reduce the system of twelve PDEs developed in section 2.3 to the following two second order PDEs for the intermediate quantities $\tilde{K}$ and $\tilde{L}$,

$$\beta^2 \frac{\partial^2 \tilde{K}}{\partial z^2} - \frac{\partial^2 \tilde{K}}{\partial t^2} = 0$$
$$\beta^2 \frac{\partial^2 \tilde{L}}{\partial z^2} - \frac{\partial^2 \tilde{L}}{\partial t^2} = 0. \tag{2.25}$$

To solve equations (2.25), we try solutions of the form

$$\tilde{K}(z,t) = e^{\lambda_1 z} M(t)$$
$$\tilde{L}(z,t) = e^{\lambda_2 z} N(t)$$

where $\mathcal{R}e\{\lambda_1\} > 0$, $\mathcal{R}e\{\lambda_2\} < 0$ are needed for stability, and $M(t)$, $N(t)$ are unknown functions of t. One can then obtain the forms of the vertical velocities,

$$\hat{w}_1(z,t) = e^z A_1(t) + e^{\lambda_1 z}\left[\frac{c_1 \cosh \beta\lambda_1 t + c_2 \sinh \beta\lambda_1 t}{\lambda_1^2 - 1}\right]$$
$$\hat{w}_2(z,t) = e^{-z} A_2(t) + e^{\lambda_2 z}\left[\frac{d_1 \cosh \frac{\beta\lambda_2}{\sqrt{D}} t + d_2 \sinh \frac{\beta\lambda_2}{\sqrt{D}} t}{\lambda_2^2 - 1}\right],$$

where $A_1(t)$, $A_2(t)$ are unknown functions of t, and c_1, c_2, d_1, d_2, λ_1 and λ_2 are unknown constants, all eight of which can be obtained by use of the boundary, interface and initial conditions. In the special case that $\lambda_1 = 1$ or $\lambda_2 = -1$, then the above are evaluated in the limit. We use the interface conditions (2.15) and the initial conditions (2.18) to solve for the required constants. Of particular interest here are the quantities λ_1 and λ_2. It may be shown that, in order to satisfy the interface and initial conditions, we require the following relationship between λ_1 and λ_2, and we thus define the new quantity λ by,

$$\lambda = \sqrt{D}\lambda_1 = -\lambda_2.$$

Again, the quantity of main interest is the profile of the interface, given by,

$$\eta(x,t) = \epsilon \cosh\left(\sqrt{\mathcal{A}_{m_\perp}}t\right)\cos x + O\left(\epsilon^2\right), \tag{2.26}$$

where the magnetic Atwood number for the field perpendicular to the interface is given by,

$$\mathcal{A}_{m_\perp} = \beta^2\lambda^2. \tag{2.27}$$

All that remains is to calculate the value for growth rate λ. It may be shown that the initial conditions (2.18) and interface conditions (2.15) lead to the following cubic equation, from which λ is obtained,

$$\beta^2(D+1)\lambda^3 + 2\beta^2\left(\sqrt{D}+1\right)\lambda^2 + \left(1 - D + 2\beta^2\right)\lambda + 2\left(1-\sqrt{D}\right) = 0, \tag{2.28}$$

in which we require $\mathcal{R}e\{\lambda\} > 0$ for stability. It can be shown with elementary methods as well as Descartes Rule of Signs (see [37]) that the cubic (2.28) has exactly one positive root, and hence that root must also be real. It can also be shown in the limit of no magnetic field that we recover the original Atwood number for the growth rate of the interface, as in Forbes [24].

2.3.3 Arbitrary Base Field

In this final case, our base magnetic field is directed at some angle to the interface, and has the expression $\boldsymbol{B_1} = \boldsymbol{B_2} = \beta\left(l_x \hat{\boldsymbol{e}}_{\boldsymbol{x}} + l_z \hat{\boldsymbol{e}}_{\boldsymbol{z}}\right)$, where l_x and l_z are direction cosines as defined in equation (2.13). Again, the dimensionless constant β represents the ratio of the base magnetic flux density to the reference flux density $\sqrt{\mu_1 \lambda \rho_1 g/2\pi}$. It is straightforward to use the superposition principle to obtain the solution in this case for the interface to be

$$\eta\left(x,t\right) = \epsilon\left(l_x \cosh\sqrt{\mathcal{A}_{m_{||}}}t + l_z \cosh\sqrt{\mathcal{A}_{m_{\perp}}}t\right)\cos x + O\left(\epsilon^2\right), \tag{2.29}$$

where $\mathcal{A}_{m_{||}}$ and $\mathcal{A}_{m_{\perp}}$ are defined in equations (2.24) and (2.27) respectively.

This result is in agreement with a similar result derived under slightly different conditions by Chandrasekhar [13].

2.4 Discussion and Conclusion

The main result from this chapter is equation (2.29), which governs the time evolution of interfacial waves in the case of the MRTI. This, in conjunction with the magnetic Atwood numbers for horizontal and vertical base magnetic fields given in equations (2.24) and (2.27) respectively, allows the location of the interface to be calculated at a point in time, accurate to first order in terms of the wave amplitude. These interface locations will be shown graphically in the results of the next chapter, where they will be of great use in allowing the numerical non-linear solutions to be verified at early time periods, that is, where the linear solution is valid. Several figures are presented in which a superposition of the linear and non-linear solutions is given at certain snapshots in time. A comparison is made for all three cases of horizontal, vertical and angled base magnetic fields, and the results compare favourably. This in turn gives confidence that the numerical methods of the next chapter are stable and accurate. A summary of possible behaviours for the various cases in now given.

In the case of a horizontal base magnetic field, there are three different types of behaviour depending on the sign of the magnetic Atwood number given by equation (2.24). Very weak magnetic fields give rise to an Atwood number that is positive, and thus the growth rate is exponential, and comparable with the case of no magnetic field. There is a critical value for the strength of the magnetic field in which the magnetic Atwood number is 0. The growth rate of the interface is thus fully suppressed in time in this case. Magnetic fields stronger than this critical value will thus result in a negative magnetic Atwood number, and the behaviour of the interface will be oscillatory in time.

The case of a vertical base magnetic field is somewhat more difficult to analyse given the more complicated form of the magnetic Atwood number in equation (2.27). There are, however, the same three types of behaviour as for the horizontal magnetic field case. What is more difficult is calculating in general the density ratio and magnetic field strength to give each type of behaviour. This is due in part to the requirement of finding the one positive root of a cubic equation (2.28) which has coefficients that are combinations of the density ratio and magnetic field strength.

The linear nature of the solution under consideration allows a complete description of the response due to an angled field to be described by a superposition of the behaviours in the horizontal and vertical magnetic field cases. We conclude with some analytic consequences of the calculated magnetic Atwood numbers. Firstly, in each case, it can be seen that the magnetic Atwood number depends on the square of the magnetic field strength. The result of this is that the growth rate of the interface is independent of the polarity of the magnetic field. Finally, it is important that the magnetic Atwood numbers calculated in this paper give identical growth rates to the well known Atwood number in the case of no magnetic field. This is trivial to see in the horizontal case, but more difficult to verify in the vertical case, where a complicated limit is required, but does indeed give the correct value.